Chapter 2
Fundamentals of FT-IR

2.1 Principle of Spectral Measurements

A schematic of IR spectroscopy is illustrated in Fig. 2.1, which presents the physical fundamental of spectroscopy. The IR source emits IR ray, and a portion of the ray through the slit is made a parallel light by mirrors (omitted in the figure), $I(t)$, going to the prism.

At the moment, the light has an image of the plane wave of electric and magnetic fields as a function of time, t, and the intensity, I, is proportional to the squared electric field (Eq. 3.17). The prism is an optical element working as the heart of the spectrometer: the refraction angle depends on the wavelength of the light. In this manner, the straight parallel light becomes a "dispersed" light. If the light is visible light, a rainbow pattern appears on the screen. Since the IR light is invisible, an IR detector must be used to have a spectrum instead of the visible pattern.

The spectrum appears as a graph developed by two axes of wavelength, λ, and intensity, S. Since the wavelength is directly interrelated with a more useful parameter, angular frequency (ω), the spectrum is denoted as $S(\omega)$ in the figure. In this manner, the optical element works to transform the time-domain function, $I(t)$, to the frequency-domain one, $S(\omega)$, which corresponds to Fourier transform in mathematics. In other words, the role of the optical element is Fourier transform the light to a spectrum very quickly with the light velocity. Regardless, this type of spectrometer using an optical dispersive element is *not* called a Fourier transform spectrometer, but a dispersion-type spectrometer.

Fourier transform is represented by a pair of equations.

$$S(\omega) = \int_{-\infty}^{\infty} I(t)\mathrm{e}^{-\mathrm{i}\omega t}\,\mathrm{d}t \tag{2.1}$$

T. Hasegawa, *Quantitative Infrared Spectroscopy for Understanding of a Condensed Matter*, DOI 10.1007/978-4-431-56493-5_2

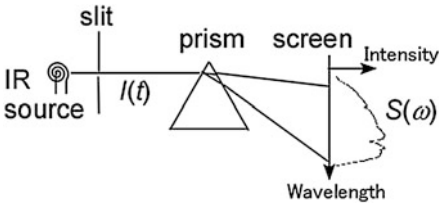

Fig. 2.1 Schematic of a dispersion-type spectrometry

$$I(t) = \frac{1}{2\pi} \int_{-\infty}^{\infty} S(\omega) \mathrm{e}^{\mathrm{i}\omega t} \, \mathrm{d}\omega \tag{2.2}$$

Equation (2.2) is especially easy to understand intuitively. Since $\mathrm{e}^{\mathrm{i}\omega t}$ represents an oscillation like a cosine wave, the summation of the waves with the weighting function of $S(\omega)$ for all frequencies yields the time-domain representation of the broadband wave, $I(t)$. This equation is called "inverse Fourier transform." The role of the prism in Fig. 2.1 is represented by the Fourier transform: $I(t)$ is transformed to $S(\omega)$. If $I(t)$ is readily measured, the spectrum is thus obtained by calculation using Eq. (2.1) *without using an optical element like a prism*, which is called *Fourier transform spectrometry*.

A dispersion-type spectrometer has experimental limitations as follows.

(1) If the refraction (or diffraction) angle-variance is highly limited by using a narrow slit, the wavenumber resolution becomes high. This spatially limited light is, however, very dark, which results in a poor quality spectrum.
(2) To obtain a spectrum, a mechanical scanning of wavelength is necessary. A perfect reproducibility of mechanical scanning cannot be expected, and the calibration of the abscissa axis is necessary for each measurement. Therefore, reliable accumulation of spectra for improving spectral quality is generally difficult.
(3) The spectral quality depends on the speed of the mechanical scanning. To have a high-quality spectrum, a slow scanning is required, which takes much time. In other words, only a stable sample can be measured.

These intrinsic matters specific to a dispersive-type spectrometer can totally be overcome by introducing the Fourier transform (FT) technology in theory.

Nevertheless, a direct measurement of $I(t)$ requires a very high technique, since ultrafast measurements are necessary. Mid-IR light is generally recognized as the wavenumber range of 4000–400 cm^{-1}, which corresponds to the wavelength region of ca. $\lambda = 10\,\mu\mathrm{m}$, which further corresponds to $\nu = 30$ THz = 3×10^{13} Hz ($c = \nu\lambda$). To measure the IR light in the time-domain, therefore, an ultrafast spectrometer having a time resolution of ca. 3×10^{-14} s (femtosecond region) is necessary. In other words, a femtosecond pulse laser must be employed for obtaining an IR spectrum to straightforwardly employ the FT principle, which needs much cost and a very high measurement skill.

To get over the technical difficulty, an alternative great idea is employed using an interferometer.

2.2 Introducing an Interferometer: FT-IR

For IR measurements, a unique optics is introduced to realize the FT spectrometry preventing the ultrafast measurements. The optics is an *interferometer* represented by Michelson's one as illustrated in Fig. 2.2.

The interferometer consists of a beam splitter and two plane mirrors. The beam splitter allows a half of the light pass through it, and the rest half is reflected on the surface. One of the mirrors is placed at a fixed position with a distance of x_1 to the splitting point, whereas the other mirror is on a rail to change the distance, x_2, which is called the "moving mirror." The moving mirror is moved very smoothly with an electronically controlled highly constant velocity, v_m.

When the moving mirror is displaced from the initial position of $x_2 = x_1$ with the constant velocity of v_m, the position of the moving mirror, $x_2(t)$ is represented as

$$x_2(t) = x_1 + v_m t.$$

A parallel IR ray is led to the interferometer, a half of the light goes to the fixed mirror, and the reflected light is half reflected on the splitter to go as output. In a similar manner, the rest half is reflected to go to the moving mirror, and the reflected light goes through the splitter to go as output. As a result, the two lines of light are overlaid in the output path, which generates interference.

The superposition of the two electric field oscillation waves, $E(t)$, can simply be expressed by considering three facts. (1) the amplitudes, A, of the two waves are the same as each other, since the beam splitter splits the light for the transmission and the reflection half-and-half, (2) the angular frequency, ω, is common to the two waves, and (3) a round trip between the beam splitter and a mirror influences the phase change. The superposition is thus simply expressed by Eq. (2.3).

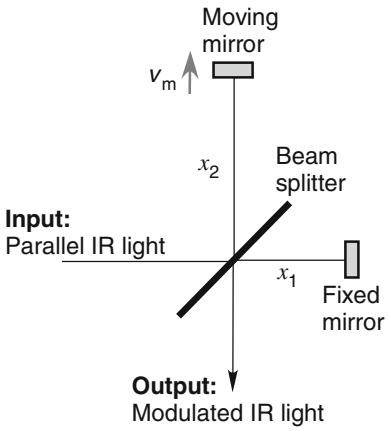

Fig. 2.2 A top-view schematic image of Michelson's interferometer

$$\begin{aligned} E(t) &= A\ \exp \mathrm{i}(2kx_1 - \omega t) + A\ \exp \mathrm{i}(2kx_2 - \omega t) \\ &= A[\exp \mathrm{i}(2kx_1 - \omega t) + \exp \mathrm{i}\{2k(x_1 + v_\mathrm{m} t) - \omega t\}] \\ &= A\{\exp \mathrm{i}(2kx_1 - \omega t)\}(1 + \exp \mathrm{i}2kv_\mathrm{m} t) \end{aligned} \tag{2.3}$$

The light "intensity" measured by the detector is the energy flow of the electromagnetic wave (Poynting vector in Sect. 3.3), which is proportional to the squared absolute value of the electric field. Therefore, the light intensity is calculated using Eq. (2.3) as:

$$\begin{aligned} |E|^2 &= E^* E = A^2(1 + \exp(-\mathrm{i}2kv_\mathrm{m} t))(1 + \exp \mathrm{i}2kv_\mathrm{m} t) \\ &= 2A^2(1 + \cos 2kv_\mathrm{m} t) \\ &= 2A^2(1 + \cos 2\pi f t) \end{aligned} \tag{2.4}$$

Here, the frequency, f, is obtained by considering $k = 2\pi/\lambda = 2\pi\tilde{\nu}$:

$$2\pi f = 2kv_\mathrm{m} \Leftrightarrow \boxed{f = 2\tilde{\nu} v_\mathrm{m}}. \tag{2.5}$$

This frequency is called "*modulation frequency*."

Here, $\tilde{\nu}$ is the wavenumber of the original IR light, which has a wide range from 400 to 4000 cm^{-1}. To consider the modulation frequency simpler, the wavenumber of He–Ne laser is conveniently used "as a constant" instead of using that of broadband IR. Since the wavelength of the laser is 632.816 nm in air, the wavenumber is calculated to be:

$$\tilde{\nu} = 1/\lambda = 15{,}802.4\,\mathrm{cm}^{-1}.$$

When the mirror velocity is $v_\mathrm{m} = 1.8984$ cm s^{-1}, for example, the modulation frequency is thus calculated to be $f = 60.0$ kHz. In other words, by introducing the wavenumber as a constant, *the mirror velocity can be interpreted to be the modulation frequency*. The scientific community of FT-IR has a tradition to write the modulation frequency instead of mirror velocity in a research paper.

When a wavenumber of IR light is put in Eq. (2.5), the modulation frequency becomes about 1 kHz, which is significantly smaller than the original IR frequency by about 1×10^{10} Hz. Therefore, the very fast oscillation of the electric field of IR light is invisible on the modulated IR light. Thanks to the low frequency of the modulated light, high-sensitive IR detectors are readily employed for FT-IR. Pyroelectric and semiconductor sensors are the representatives.

(1) Pyroelectric sensor

Deuterated triglycine sulfate (DTGS) has a character that the polarity on the surface changes on irradiation of IR light (or heat) via a molecular orientation change. Since the molecular orientation change happens in a millisecond range, a DTGS detector

responds to an electric oscillation at most a kHz order. The modulated IR light is quite suitable to employ the detector fortunately.

Since a thermal "variation" induces the surface charge, the background stable heat (ambient temperature) does not influence the output. Therefore, a DTGS detector works at an ambient temperature. This is a great benefit of using this detector. On the other hand, the sensitivity depends on the rate of molecular orientation change. In other words, the modulation frequency (or mirror velocity) is a dominant factor to influence the sensitivity. In general, a lower modulation frequency yields a high sensitivity, although the measurement time becomes longer. This technique is particularly useful to measure a very weakly absorbing sample. 5 kHz (i.e., $v_m = 0.15820$ cm s^{-1}) is a representative modulation frequency for high-sensitive measurements, although one scan needs a long time of about 4 s.

Since this detector is inferior to the MCT detector in sensitivity, DTGS is often selected for a bright (high throughput) measurement represented by reflection absorption (RA) and transmission spectrometries (Chap. 3).

(2) Semiconductor sensor

An alloy of mercury, cadmium, and telluride (MCT) works as a semiconductor sensor for IR light: an electron in the valence band is excited to be a free electron in the conduction band by absorbing the IR light. Since the ambient temperature contributes to the excitation, the detector must be cooled down to a working temperature using liquid nitrogen (LN_2). The container of LN_2 is covered by a Dewar bin, which must be vacuumed adequately; otherwise the duration time becomes very short.

An MCT detector has a wide frequency range, and the sensitivity does not respond to the modulation frequency significantly. The sensitivity is much higher than that of a DTGS one by one order of magnitude and it is thus suitable for detecting a low throughput measurement such as external reflection (ER) and attenuated total reflection (ATR) measurements (Chap. 3). Although MCT can also be used for RA and transmission measurements, a metal-mesh filter (light attenuator) must be placed in the light path to prevent the signal saturation of the detector.

Let us get back to Eq. (2.4). $A(\tilde{\nu})^2$ is the observed light intensity, and therefore it can be replaced by a spectral pattern, $S(\tilde{\nu})$. In addition, another replacement of $x \equiv 2v_m t$ is introduced, with which the time-domain measurements are converted to the measurements on the mirror position. Since the mirror position is precisely controlled electromecanically, the position is accurately read. In this manner, the following measurements at a wavenumber of $\tilde{\nu}$ are readily carried out.

$$A^2 \cos 2\pi 2\tilde{\nu} v_m t = S(\tilde{\nu}) \cos 2\pi \tilde{\nu} x$$

In practice, this measurement is performed for a broadband IR light, which results in $I(x)$ as:

$$I(x) \equiv \frac{2}{\pi} \int_0^\infty S(\tilde{\nu}) \cos 2\pi \tilde{\nu} x \, \mathrm{d}\tilde{\nu}. \tag{2.6}$$

An example of the observed *interferogram*, $I(x)$, is presented in Fig. 2.3. Note that the interferogram is the "raw experimental data" on FT-IR. Equation (2.6) has a formation of the even-function part of the Fourier transform, and thus $S(\tilde{\nu})$ is pulled out by performing the FT calculation as Eq. (2.7).

$$S(\tilde{\nu}) = 2 \int_0^\infty I(x) \cos 2\pi \tilde{\nu} x \, \mathrm{d}x \tag{2.7}$$

In this fashion, an ultrafast measurement in the time domain is readily avoided by introducing the interferometer. This technique is accomplished thanks to a good detector working in a low-frequency range, which fortunately corresponds to the modulation frequency.

This lucky holds for the mid- and near-IR regions. In other words, the FT technology employing the interferometer is not used for the UV-vis region. This is a reason why no FT-Vis is commercialized, which is another reason why no FT-Raman spectrometer with a visible excitation-laser is available.

2.3 Laser and FT Spectrometer

In an FT-IR spectrometer, a He–Ne laser optics is equipped as well as the IR optics: the laser-beam path is parallel to the IR path in the interferometer, and a laser detector is also available near the exit of the interferometer (Fig. 2.4). As described for the modulation frequency, a He–Ne laser is conveniently used to determine the frequency of the modulated IR light. To understand the necessity of the laser, the interrelationship between the time- and frequency-domain functions should be understood.

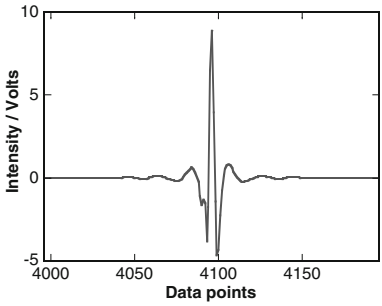

Fig. 2.3 An interferogram measured by FT-IR. This curve is subjected to the inverse FT calculation to obtain an IR spectrum

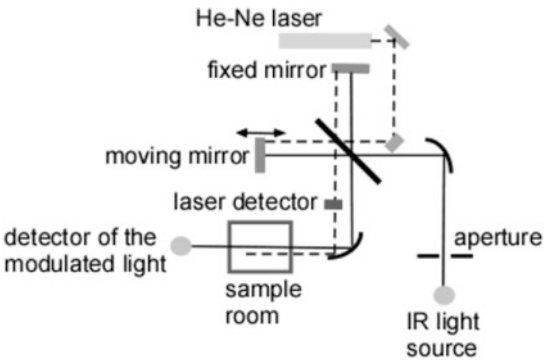

Fig. 2.4 A schematic view of the optics of IR (*solid line*) and laser (*dashed line*) light paths

(1) When $I(x)$ is the interferogram of IR broadband light:

The IR source emits broadband IR light that covers entire wavenumber range of mid-IR (4000–400 cm^{-1}). To make the discussion simpler, no intensity variation is assumed, and a simple boxcar function is considered.

The boxcar function, $S(\omega)$, illustrated in Fig. 2.5 is mathematically described as:

$$S(\omega) = \begin{cases} 1 & (0 \leq \omega \leq \omega_0) \\ 0 & (\omega < 0,\ \omega > \omega_0) \end{cases}$$

To apply this function to Eq. (2.6), the complex FT calculation is performed and the real part is extracted.

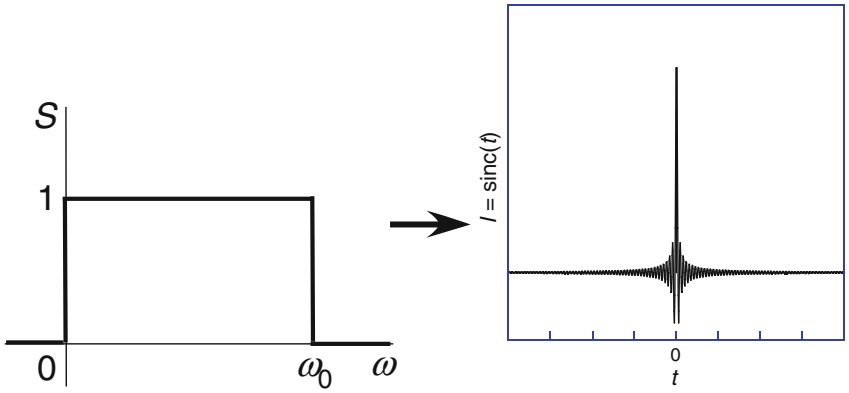

Fig. 2.5 Fourier transform of a box function to have an interferogram

$$\begin{aligned}\mathrm{Re}\left[\int_{-\infty}^{\infty} S(\omega)\mathrm{e}^{-\mathrm{i}\omega t}\mathrm{d}\omega\right] &= \mathrm{Re}\left[\int_{0}^{\omega_0} \mathrm{e}^{-\mathrm{i}\omega t}\mathrm{d}\omega\right] = \mathrm{Re}\left(\frac{\mathrm{i}}{t}\left[\mathrm{e}^{-\mathrm{i}\omega t}\right]_0^{\omega_0}\right) \\ &= \mathrm{Re}\left[\frac{\mathrm{i}}{t}\left(\mathrm{e}^{-\mathrm{i}\omega_0 t} - 1\right)\right] \\ &= \frac{\sin\omega_0 t}{t} = \omega_0 \,\mathrm{sinc}\ \omega_0 t\end{aligned} \tag{2.8}$$

This calculated result, which can be expressed using the "sinc" function (Eq. 2.8), is plotted in the right panel of Fig. 2.5. The sinc function provides a typical shape of a "wave packet," which has a center burst and decreasing envelopes for both sides. In this manner, the origin (center position) of the interferogram is accurately determined experimentally using the center burst after the measurements of the IR broadband light.

Note that even a simple calculation yields a fairly similar interferogram to the observed one presented in Fig. 2.3.

(2) When $I(x)$ is the interferogram of the He–Ne laser light:

On the contrary, what would happen, if the input light is given by a laser that has a single frequency? This case is expressed as: $S(\omega)$ has a needle-like peak at $\omega = \omega_0$ only. This situation is approximately theorized by using Dirac's delta function. On referring to a character of the Delta function (Eq. 4.9), the cosine function is obtained as the Fourier transform of Dirac's delta function (Eq. 2.9).

$$\mathrm{Re}\left[\int_{-\infty}^{\infty} \delta(\omega - \omega_0)\mathrm{e}^{-\mathrm{i}\omega t}\mathrm{d}\omega\right] = \mathrm{Re}\left(\mathrm{e}^{-\mathrm{i}\omega_0 t}\right) = \cos\omega_0 t \tag{2.9}$$

This means that the interferogram of a laser light becomes a cosine curve.

In short, when a laser light is input into the interferometer, a cosine-shaped wave is generated as the interferogram, as already shown by Eq. (2.4). This cosine shape can be used as graduation marks of the interferogram.

With the characteristics of (1) and (2), the origin and the graduation marks of the interferogram are both accurately determined by the simultaneous measurements of IR broadband light and a laser. Therefore, a laser light is a necessary item for FT-IR, and we need no calibration for the abscissa axis of the final output (cm^{-1}). This high accuracy of abscissa is a great benefit of using FT spectroscopy.

As shown in Fig. 2.4, the laser detector is placed near the exit of the interferometer "before" the sample room. In general, the laser detector allows a portion of the laser light pass through the laser detector, which attains the sample room. Since the IR light is invisible, this "leaked" red laser light is quite useful to consider the light path especially for optical alignment. Note that the laser light has already been detected, and the leaked red light can be interrupted by an opaque sample.

2.4 Apodization Function

The inverse FT calculation is, in theory, performed using Eq. (2.7). Here, we have to pay an attention to the integral range from 0 to $+\infty$. Since the integral is carried out in terms of x (mirror position), the integral range means that the moving mirror moves over an infinitely large distance. In practice, however, a long retardation (i.e., $x_2 - x_1$) is a technically difficult, and it is not necessary for a practical wavenumber resolution for a condensed matter. Although a single molecule in vacuum exhibits a very sharp absorption band, a condensed matter yields a relatively broad band due to the variety of molecular interactions. In practice, the resolution of 4 cm^{-1} is adequate, which needs a retardation of 0.25 cm (=1/4 cm^{-1}) in theory. In this manner, the moving mirror moves in a distance of ca. 5 mm, which is significantly smaller than the length theoretically expected. This discrepancy between the theory and the practical measurements is expressed using the truncation function, $D(x)$.

$$D(x) = \begin{cases} 1 & (0 \le x \le L) \\ 0 & (x > L) \end{cases} \quad \text{(a boxcar window)}$$

With this window function, the integral in a limited range up to L can be written as in the original form.

$$\begin{aligned} S_D(\tilde{\nu}) &= 2\int_0^L I(x)\cos 2\pi\tilde{\nu}x \, \mathrm{d}x \\ &= 2\int_0^\infty I(x)D(x)\cos 2\pi\tilde{\nu}x \, \mathrm{d}x \end{aligned} \tag{2.10}$$

In other words, the observed FT-IR spectrum, $S_D(\tilde{\nu})$, involving the truncation function is different from the ideal spectrum, $S(\tilde{\nu})$. Equation (2.10) has a form of *FT of a function product* of $I(x)$ and $D(x)$, which is a *convolution* (see Sect. 4.2) of $\mathscr{F}[I(x)]$ and $\mathscr{F}[D(x)]$ where '$\mathscr{F}$' is the Fourier transform operator.

$$\begin{aligned} \int_0^\infty I(x)D(x)\cos 2\pi\tilde{\nu}x \, \mathrm{d}x &\equiv \mathscr{F}[I(x)D(x)] \\ &= \mathscr{F}[I(x)] * \mathscr{F}[D(x)] \\ &= \frac{1}{2\pi}\int_{-\infty}^{\infty} \mathscr{F}[I(u)] \cdot \mathscr{F}[D(x-u)]\mathrm{d}u \end{aligned}$$

Here, * denotes the convolution.

As shown by Eq. (2.8) and Fig. 2.5, $\mathscr{F}[D(x)]$ (sometimes called "*instrumental line shape* (*ILS*) *function*") has a shape of the sinc function that has a many fringe-like tails on both sides of the main peak. Therefore, the fringes of the sinc function should influence the final spectrum, $S_D(\tilde{\nu})$.

To remove the fringes, the boxcar function, $D(x)$, is modified to have another window function, $A(x)$. By replacing $D(x)$ with $A(x)$, the fringe-like oscillations can largely be reduced, and this fringe-reduction effect is called "apodization," and therefore $A(x)$ is called an "apodization function." An apodization function has a side effect that the wavenumber resolution and intensity linearity are degraded [1]. The suppression of the oscillation and the degradation are trade-off with each other.

At any rate, the selection of an apodization function is necessary to use FT-IR. Many apodization functions have been proposed thus far. The representative functions are: triangular, trapezoidal, cosine and Happ–Genzel functions. For the detail, the reader is referred to the literature elsewhere [1]. Once an apodization function is selected, the user should not change the function for a series of measurements; otherwise the spectra lose consistency.

Reference

1. P.R. Griffiths, J.A. de Haseth, *Fourier Transform Infrared Spectroscopy*, 2nd edn. (Wiley, Hoboken, NJ, 2007)

http://www.springer.com/978-4-431-56491-1

Quantitative Infrared Spectroscopy for Understanding of a Condensed Matter

Hasegawa, T.

2017, XI, 200 p. 115 illus., 55 illus. in color., Hardcover
ISBN: 978-4-431-56491-1